TURUN YLIOPISTO

Lymph-derived soluble Clever-1

Effect on cancer cell viability

Biolääketieteen laitos, Turun yliopisto
Medicity Research Laboratory, Hollmén group, Biocity
Syventävien opintojen kirjallinen työ
Kevätlukukausi 2023

Laatija:
Matias Knuuti

Ohjaaja:
Dos. Maija Hollmén
2.3.2023
Turku

Syventävien opintojen kirjallinen työ

Oppiaine: Lääketieteellinen mikrobiologia ja immunologia
Tekijä: Matias Knuuti
Otsikko: Lymph-derived Clever-1: Effect on cancer cell viability
Ohjaaja: Dos. Maija Hollmén
Sivumäärä: 22 sivua
Päivämäärä: 2.3.2023

Cancer is one of the most important causes of premature death. Even though the treatment of cancer has seen considerable advancements in the past decades, there are still numerous cancers without effective treatment. Metastasis and the ability of most cancers to develop resistance against cancer medicine, particularly cancer immunotherapy, hinder the efficacy of cancer treatments. One culprit in cancer immunotherapy resistance is Clever-1, which is an immunosuppressive transmembrane protein expressed on endothelial cells and macrophages. The aim of this thesis was to study how the soluble Clever-1 in human lymph affects the viability of breast cancer cells *in vitro*, to better understand the metastatic process.

Two breast cancer cell lines representing low (T47D) and high (MDA-MB-231) lymphatic metastasis capacity were chosen for the experiments. The proliferation of the cancer cells was compared between growth mediums supplemented with either Clever-1^+ or Clever-1^- human lymph. The lymph was obtained from three healthy donors and Clever-1 was depleted from the lymph by immunoprecipitation using anti-Clever-1 antibodies. The Clever-1-depletion was validated by two distinct methods: in-house Clever-1 time-resolved fluorometric immunoassay of the Clever-1-depleted lymph and by gel electrophoresis of the Clever-1 immunoprecipitate.

There was no relationship between soluble Clever-1 in lymph and the viability of the breast cancer cells. This provides important preliminary information about the roles of soluble Clever-1 in metastasis. Further studies are required on the several other steps of metastasis, such as adhesion and transmigration. Additionally, recombinant Clever-1 could be utilized to eliminate the other contents of lymph as confounding factors.

Keywords: Clever-1, metastasis, lymph, cancer

Table of contents

1 Introduction

There were almost 10.0 million deaths caused by cancer globally in 2020, and an increase of almost 50% is expected by the year 2040[1]. Even though the treatment of cancer has seen considerable advancements in the past decades, there are still numerous cancers without effective treatment. Metastasis and the ability of most cancers to develop resistance against cancer medicine, particularly cancer immunotherapy, hinder the efficacy of cancer treatments. To survive in the hostile environment of the body, cancer cells manipulate their surroundings, the tumor microenvironment (TME), leading to the upregulation of immunosuppressive signals, such as programmed death ligand 1 (PD-L1) and cluster of differentiation 47 (CD47)[2]. The TME and re-education of immune responses against cancer have been the primary focus of cancer research in recent years.

One culprit and potential target in cancer immunotherapy resistance is the Common lymphatic endothelial and vascular endothelial receptor-1 (Clever-1; also known as Stabilin-1 and FEEL-1), an immunosuppressive scavenger receptor that has been linked to the spreading of cancer and immunotherapy resistance.[3] After in situ invasion, cancer cells spread via either the blood circulation or the lymphatic system, which mainly depends on the cancer type. As a milieu for Clever-1-expression, we focused on the lymphatic system, and more precisely, lymph, as little is known about its role in metastasis.

The aim of this thesis was to study how the soluble Clever-1 in human lymph regulates cancer cell behavior and how it affects the viability of breast cancer cells *in vitro,* to better understand the metastatic process.

2 Review of the literature

2.1 Cancer metastasis

Cancer metastasis is accountable for most of the deaths related to cancer and is often considered the last stage of cancer progression. It usually takes a considerable amount of time for a tumor to form a macroscopic metastatic lesion. This comes as no surprise since the process of metastasis is very inefficient. As shown in a mouse model study of injected cancer cells that survived and extravasated, only 1 in 40 were able to form micrometastases, and only 1 in 100 of those continued to grow into macroscopic tumors. In total, only 0.02% or 1 in 5000 cells injected into the circulation were able to form macroscopic tumors.[4]

However, as shown by Stephen Paget in the late 1800s, the localization of metastatic lesions is based on the migrant cells finding a favorable environment and not on the location of the primary tumor or by chance as previously thought. This was termed the 'seed and soil' hypothesis by Paget.[5] Later it has been shown that cancers begin to condition these metastasis-favorable environments, called pre-metastatic niches, quite early in their lifespan and even before the circulating tumor cells arrive. This happens via growth factors secreted by the primary tumor, which is followed by the clustering of tumor-associated cells, such as macrophages. Afterward, a metastatic niche is formed when a circulating tumor cell localizes to, extravasates, engrafts, and proliferates in the pre-metastatic niche. The newly formed micrometastasis then carries on the conditioning process of the niche.[6]

Pre-metastatic niches in lungs and bones use specific signaling to attract inflammatory monocytes and cause them to differentiate into a pro-tumorigenic subset of macrophages: metastasis-associated macrophages (MAMs).[7–9] The inflammatory monocytes themselves also promote metastasis by producing vascular endothelial growth factor A (VEGF-A). VEGF-A induces angiogenesis, but also increases vascular wall permeability, thus helping circulating tumor cells extravasate into the pre-metastatic niche.[8,10]

MAMs in turn, contribute to metastasis by several mechanisms: they promote extravasation of tumor cells[9], are highly angiogenic[11], provide the cancer cells with survival signals[12], as well as inhibit T-cell and natural killer cell-induced tumor cell cytotoxicity and apoptosis[13,14]. Perhaps most interestingly, tumor-associated macrophages (TAMs) and MAMs participate in orchestrating what is known as the epithelial-to-mesenchymal transition of the tumor cells, and the reversal back to epithelial cells at the metastatic site. This process is essential for

cancer invasion and is what enables the dormancy of cancer cells, which helps them escape immunosurveillance.[15]

2.2 Cancer metastasis and the lymphatic system

Several nonlymphoid solid cancers, such as melanoma, colorectal cancer (CRC), breast cancer, head and neck cancer as well as many gynecological cancers spread via the lymphatic system. The lymphatic vessels are utilized as an alternative to blood vessels and usually, in these types of cancers the primary site of metastasis is found in the tumor-draining lymph nodes, specifically the sentinel lymph nodes. Thus, the removal of tumor-draining or sentinel lymph nodes has been utilized for several decades in breast cancer and melanoma surgery, to reduce the risk of relapse. In the early 2000s however, it was discovered that lymphatics have an active role in cancer metastasis, contrary to what was previously thought[18].

Firstly, it has been shown that cancer induces lymphangiogenesis, the growth and proliferation of lymphatic vessels, by expressing VEGF-C. VEGF-C interacts with lymphatic endothelial cells (LECs), mainly through its receptor VEGFR-3. The generation of novel lymphatic vessels and dilation of existing lymphatic capillaries and vessels leads to increased lymphatic drainage from the primary tumor site into the tumor-draining lymph nodes and promotes metastasis.[19,20] In fact, abundant intratumoral lymphatics are associated with metastatic disease and poor outcome, which has been shown in multiple studies on melanoma, breast, colorectal, and lung cancer.[18,21,22]

Secondly, tumor-associated LECs seem to inhibit anti-tumor T-cell responses via PD-L1 signaling. This is likely the same mechanism that LECs in lymph nodes use to maintain peripheral tolerance, hijacked by cancer cells.[23] Finally, via mouse metastasis models, it has been shown that lymphangiogenesis occurs in distant lung metastases and LECs seem to contribute to further metastasis of distant metastases.[24]

2.3 Clever-1 and cancer

Clever-1 is a transmembrane protein (molecular mass 270–280 kDa) expressed by lymphatic and vascular endothelial cells and macrophages[3]. It has been identified to have an immunosuppressive role in both physiology and pathology[25]. While the expression of Clever-1 is not seen on vascular endothelium in nonlymphoid organs physiologically, it has been shown to be upregulated during inflammation. Clever-1 acts as both an adhesion and a

scavenging molecule. As an adhesion molecule, it mediates lymphocyte trafficking for example via high endothelial venules (HEVs) of lymphoid organs. In addition, it mediates the transmigration of leukocytes, such as peripheral blood monocytes, to inflammatory sites on both vascular and lymphatic endothelial cells. As a scavenging molecule on macrophages, Clever-1 binds both Gram-positive and Gram-negative bacteria and various endogenous proteins and metabolic end products.[3,26–28] Finally, Clever-1 is expressed on M2-polarized immunosuppressive macrophages and, contrary to normal physiology, tumor blood vessels[29].

Possibly via the functions mentioned above, Clever-1 participates in the spread and growth of cancer. On TAMs and tumor vasculature, Clever-1 propagates the transmigration of immunosuppressive leukocytes into the TME and tumor cell trafficking into the regional lymph nodes.[25,29] In fact, in human CRC patients, a high number of Clever-1^+ intratumoral lymphatic vessels seems to be more common in grade IV metastatic disease, compared to grades I-III. In addition, abundant intratumoral Clever-1^+ lymphatic vessels are associated with poor disease-specific survival in stage II CRC.[30] Clever-1^+ lymphatic vessels are also associated with lymph node metastasis in human breast cancer as well as poor survival and resistance to neoadjuvant chemotherapy in human bladder cancer.[31–33]

To further investigate the impact of Clever-1 on cancer spread, and as a prospective new treatment for cancer, Clever-1 antibodies have been developed. Both the anti-Clever-1 antibody treatment and knockout of Clever-1 inhibit primary tumor progression and metastasis growth in several mouse cancer models *in vivo*. The absence of Clever-1 also correlates with higher tumor cell apoptosis and reduced infiltration of immunosuppressive leukocytes in tumors. Targeting Clever-1 in macrophages also interestingly causes a shift from immunosuppressive type 2 macrophages to immunostimulatory type 1 macrophages.[29,34]

While the roles of lymphatic vessels and lymph nodes in promoting cancer metastasis have been demonstrated, there is a gap in knowledge about the role of lymph itself in the progression of cancer.[18,35] Shed, soluble Clever-1 has been found in human lymph and serum (unpublished results), but according to searches in PubMed, Cochrane, and Embase databases, nothing is known of its functions in body fluids. In this thesis, we focused on the role of human lymph-derived soluble Clever-1 on the viability of two different breast cancer cell lines *in vitro*, to understand how Clever-1 may support the metastasis process of cancer cells, namely viability in the lymphatic vessels during their travel to the metastatic niche.

3 Materials and methods

3.1 Clever-1 depletion of human lymph

Lymph used in the experiment was obtained as a drainage product from three different chylothorax patients (donors 1, 2, and 3) treated in Turku University hospital. The chylothoraces were formed as surgical complications, but the donors were otherwise healthy. To deplete Clever-1 from the lymph, anti-Clever-1 antibody 9-11 (InVivo Biotech, AK1013/03.1) coated cyanogen bromide Activated Sepharose 4B® immunoprecipitation beads (by Sigma-Aldrich) (CNBr beads) were used. Rat IgG2a (clone MEL14, AK1632/01.2) coated CNBr beads were used as an isotype control to produce mock depleted lymph. Lymph was Clever-1 depleted in a ratio of 14:1, i.e., to deplete 14 ml of lymph, 1 ml of antibody-coated CNBr beads were used (1 g of dry beads corresponds to 3.5 ml of swollen beads).

To prepare CNBr beads for depletion, dry beads were first weighed into 15 ml Falcon tubes and washed with 1 mM hydrochloric acid (HCl). 200 ml of HCl was used per gram of beads. The beads were centrifuged for 3 min at 200*g at room temperature (RT) between each change of reagent during the whole depletion process. The swollen beads were then washed twice with coupling buffer (0.1 M $NaHCO_3$ and 0.5 M NaCl in MilliQ water, at 8.3 pH), after which coupling buffer was added on top of the beads in a ratio of 1:1. To coat the beads with antibodies, the beads were incubated using an end-over-end (e-o-e) mixer overnight at 4 °C with either anti-Clever-1 or rat IgG2 antibodies diluted in coupling buffer. 3 mg of antibody per 1 ml of swollen beads was used. After washing the antibody-coated beads twice with coupling buffer, they were blocked with 0.1 M tris(hydroxymethyl)aminomethane-hydrochloric acid (Tris-HCl, at 8.0 pH) for 2 h e-o-e at RT to prevent unspecific adhesion. The beads were then washed with acetate buffer (0.1 M CH3COONa and 0.5 M NaCl in Milli-Q water, at 4.0 pH) and Tris-buffer (0.1 M Tris-HCl and 0.5 M NaCl in Milli-Q water) by turns in respective order, in total 3 times for both solutions. The ready-to-use beads were suspended in phosphate-buffered saline (PBS).

The depletion of the lymph consisted of three rounds of bead incubations, each one using one-third of the antibody-coated beads. The first was for 4 h e-o-e at RT, the second overnight e-o-e at 4 °C, and the third 2 h e-o-e at RT. PBS was removed from the beads before use and the beads were suspended in lysis buffer (2% Triton X-100, 0.15 M NaCl, 10 mM Tris-Base, and 1.5 mM $MgCl_2$ x $6H_2O$ in MilliQ water). The depleted lymph was diluted 1:9 in RPMI-1640

HEPES modification (R5886 by Sigma-Aldrich) with GlutaMAX™ (by Thermo Fisher), filtered for cell culture use using Millex®-GS 0.22 µm Sterile filters (Merck Millipore Ltd.) and frozen at -18 °C.

3.2 Validation of the Clever-1 depleted lymph

3.2.1 Gel blotting of the Clever-1 precipitate to validate the depletion

The used anti-Clever-1-coated beads of donor 4 were washed 10 times with lysis buffer. They were then moved into an Eppendorf tube and 800 µl of ice-cold MQ H_2O was added on top and the solution was mixed carefully. The MQ H_2O was then removed by centrifugation (105 x g at 4 °C for 3 min). The immunoprecipitated proteins were eluted by adding the volume of the beads of ice-cold triethanolamine (TEA) MQ H_20 (TEA 50 µl/10 ml) mixing carefully and centrifuging for 90 seconds at 105 g and 4 °C. The eluate was salvaged, and this step was repeated in total three times. The eluate fractions were lyophilized in a vacuum contractor for 4 h at RT and stored at 4 °C.

The dried-up protein fractions were dissolved in 30 µl of sample buffer (50 mM Tris-HCl, 2% SDS, 10 glycerol, and 0.01% Bromphenol Blue in aqua at pH 6.8) and blotted on a commercial 10-well Mini-PROTEAN TGX 4–20% gradient agarose gels (BIO-RAD). 0.25, 0.5, 1.0, 2.0, 4.0, and 8 µg of bovine serum albumin (BSA) in 30 µl of sample buffer were used as protein standards and 5 µl of Amersham™ ECL™ Full Range Rainbow™ Marker (RPN800E by GE Healthcare) was used as the molecular weight marker. The gel was stained using Coomassie Brilliant Blue G250 (by Thermo Fisher) according to the manufacturer's protocol and imaged by using an Odyssey CLx Imager (LI-COR Biosciences) (Figure 1). Additionally, the Clever-1 concentration of the lymph was estimated by computing the relative intensity of the Clever-1 band using ImageJ image analysis software version 2.9.0 and comparing it to the standard curve based on the intensities of the BSA bands. The resulting

Clever-1 concentration was 0.77 µg/ml.

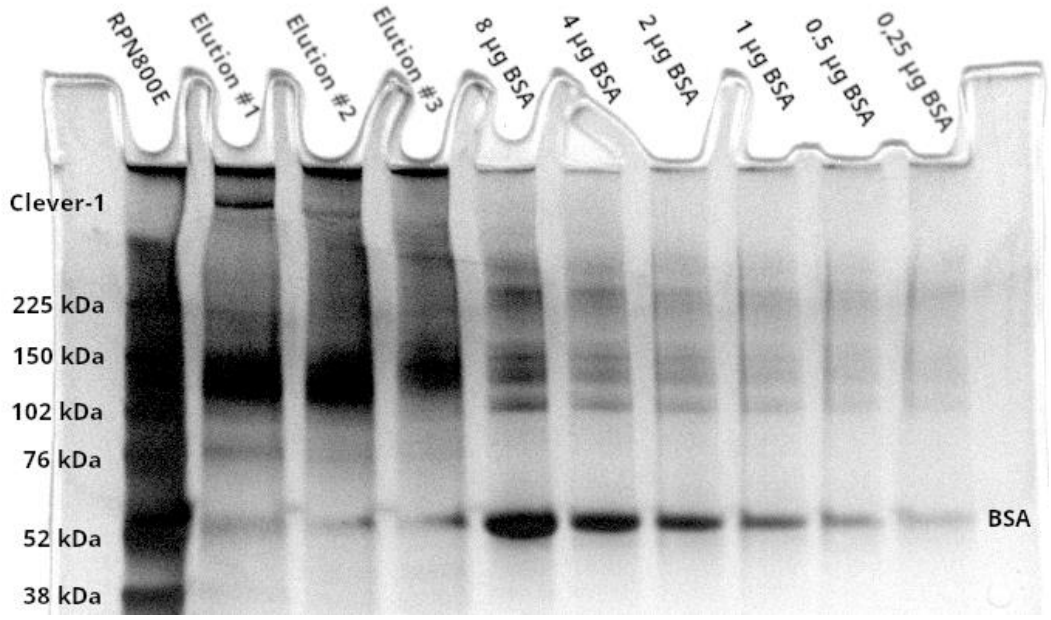

Figure 1. Coomassie Brilliant blue stained agarose gel of donor 3's Clever-1 immunoprecipitant. Elutions #1–3 on top of the image denote the elutions of the immunoprecipitant in order. The different BSA labels denote the mass of the BSA standard in each well. The locations of the Clever-1 and BSA bands are denoted by the labels *Clever-1* and *BSA*, respectively. Amersham™ ECL™ Full Range Rainbow™ Marker (RPN800E by GE Healthcare) was used as the molecular weight marker. BSA = bovine serum albumin.

3.2.2 Clever-1-TRFIA

In-house developed Clever-1-TRFIA (time-resolved fluorometric immunoassay) was used to determine Clever-1 concentrations of the differently treated batches of lymph. The assay uses two different anti-Clever-1 antibodies (9-11 and biotinylated FP1305) and europium-streptavidin as the immunolabel. A dilution series of 1:10, 1:15, 1:20, 1:40, 1:80, and 1:160 of lymph in PBS was chosen for the standard curve, as the relationship of Clever-1-concentration and TRFIA-signal was found to be linear in this dilution range. To make sure that the signal was not caused by dilution in PBS, the dilutions were also made in Clever-1-depleted lymph. Both methods produced identical standard curves (R^2: 0.993).

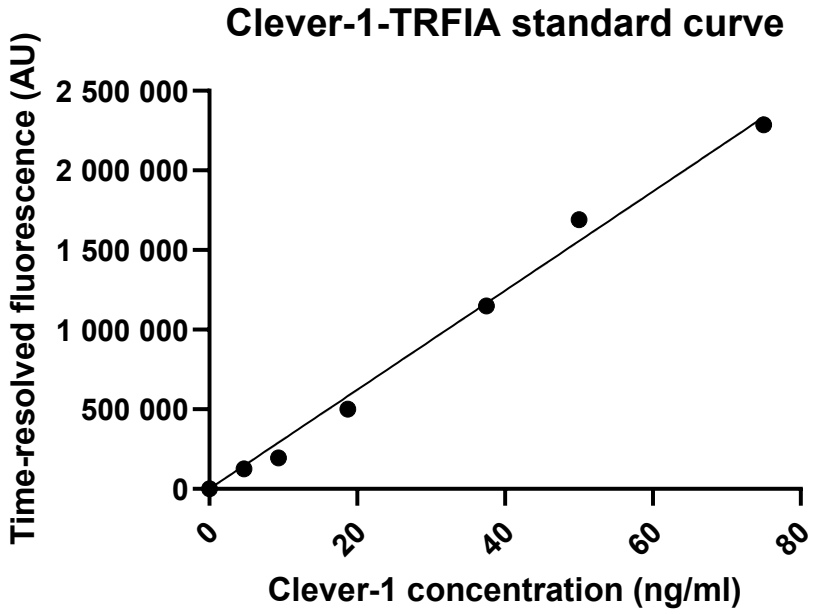

Figure 2. Time-resolved fluorescence by Clever-1 concentration plotted on a linear regression model. The points represent the dilution series of the standard lymph. TRFIA = time-resolved fluorometric immunoassay. AU = arbitrary units.

Untreated, mock-depleted, and Clever-1-depleted lymph of the donors diluted 1:20 were included in the assay. In creating the standard curve, standard lymph (donor 4 lymph with a known high Clever-1 concentration of 770 ng/ml, measurement explained in chapter 3.2.1) was used. The time-resolved fluorescence (TRF) signals of the dilution series were plotted on a linear regression model to form a standard curve showing the correlation between europium counts and Clever-1 concentration (Figure 2). The TRF signal of the Clever-1-depleted standard lymph was subtracted from the TRF signals of the other wells as background, making zero signal correspond to a null concentration of Clever-1. The Clever-1 concentrations of the lymph samples were then computed based on the slope of the dilution series. Three technical replicants were used in the assay. Extreme outliers were excluded based on visual estimation.

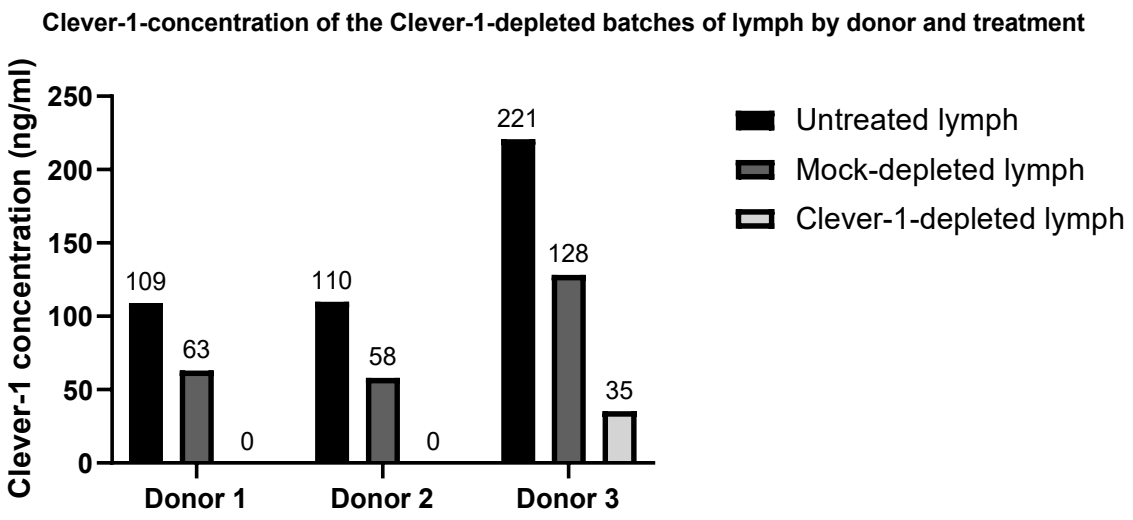

Figure 3. Clever-1-concentration of the different batches of Clever-1-depleted lymph computed based on the slope of the dilution series. Untreated lymph Negative values are marked as zero.

As seen in Figure 2, a slight decrease in Clever-1 concentration was seen even after mock-depletion of lymph, but Clever-1-depletion of donors' 1 and 2 lymph was optimal. A slight residual of Clever-1 remained in donor 3 Clever-1-depleted lymph, though there was still a marked difference compared to the mock-depleted lymph.

3.3 Viability of cancer cells and experimental protocols

3.3.1 Choosing and preparing the cell lines

Two different breast cancer cell lines representing low (T47D), and high (MDA-MB-231) lymphatic metastasis capacity were chosen for the experiments. The T47D cell line is an estrogen receptor-positive (ER+) breast adenocarcinoma cell line originally established from pleural effusion of a PR+ and ER+ ductal breast adenocarcinoma of a 54-year-old female[36,37]. Conversely, the MDA-MB-231 cell line is a spindle-like, highly aggressive, invasive, and poorly differentiated triple-negative breast adenocarcinoma cell line derived from pleural effusion of a 51-year-old Caucasian female with metastatic mammary adenocarcinoma. Both cell lines grow adherently.

The cells were purchased from the American Type Culture Collection and were tested for mycoplasma contamination using the MycoProbe kit (R&D Systems). The cells were cultured in a cell incubator, at 37°C and 5% CO_2, and appropriate methods were used in cell subculture. RPMI-1640 HEPES modification (R5886 by Sigma-Aldrich) (RPMI)

supplemented with 10 % fetal bovine serum (FBS) and GlutaMAX™ (by Thermo Fisher), was used as the growth medium for both cell lines.

For the experiment, cells were plated on Incucyte® ImageLock 4379 (Essen BioScience) 96-well plates, 5 000 MDA-MB-231 cells, and 10 000 T47D cells in each well. The cell numbers were selected based on the proliferation rates of the cell lines. A Neubauer improved cell count chamber was used to determine cell count estimates. After 6 – 12 hours of attachment, the growth medium was replaced with starvation medium (RPMI supplemented with GlutaMAX™). The cells were starved overnight, after which the medium was replaced with treatment medium. Four different treatments were used: starvation medium (negative control), regular growth medium (positive control), growth medium with the FBS replaced by 10 % mock-depleted lymph (Clever-1^{+}), and growth medium with FBS replaced by 10% Clever-1 depleted lymph (Clever-1^{-}). Five technical replicates were used.

Cell confluence in relation to time was measured by Incucyte® ZOOM Live-Cell Analysis System by Essen Bioscience (Incucyte). Incucyte was set up to take a phase contrast image of every well every two hours. Cell confluence was estimated using an algorithm trained with sample images of cells from both cell lines in different confluences. The parameters were then manually fine-tuned so that the program's confluence mask (shown in Figure 3) best corresponded to visually estimated cell borders. An additional set of images was then used to test the fitness of the confluence mask.

After culturing the cells in Incucyte, the medium was removed from the wells and the plates were frozen at -40 °C. The relative cell number of each well was then estimated by using the CyQuant™ Cell Proliferation Assay kit by Thermo Fisher (CyQuant) according to protocol. The kit uses fluorescence to determine DNA concentration, which correlates to cell number.

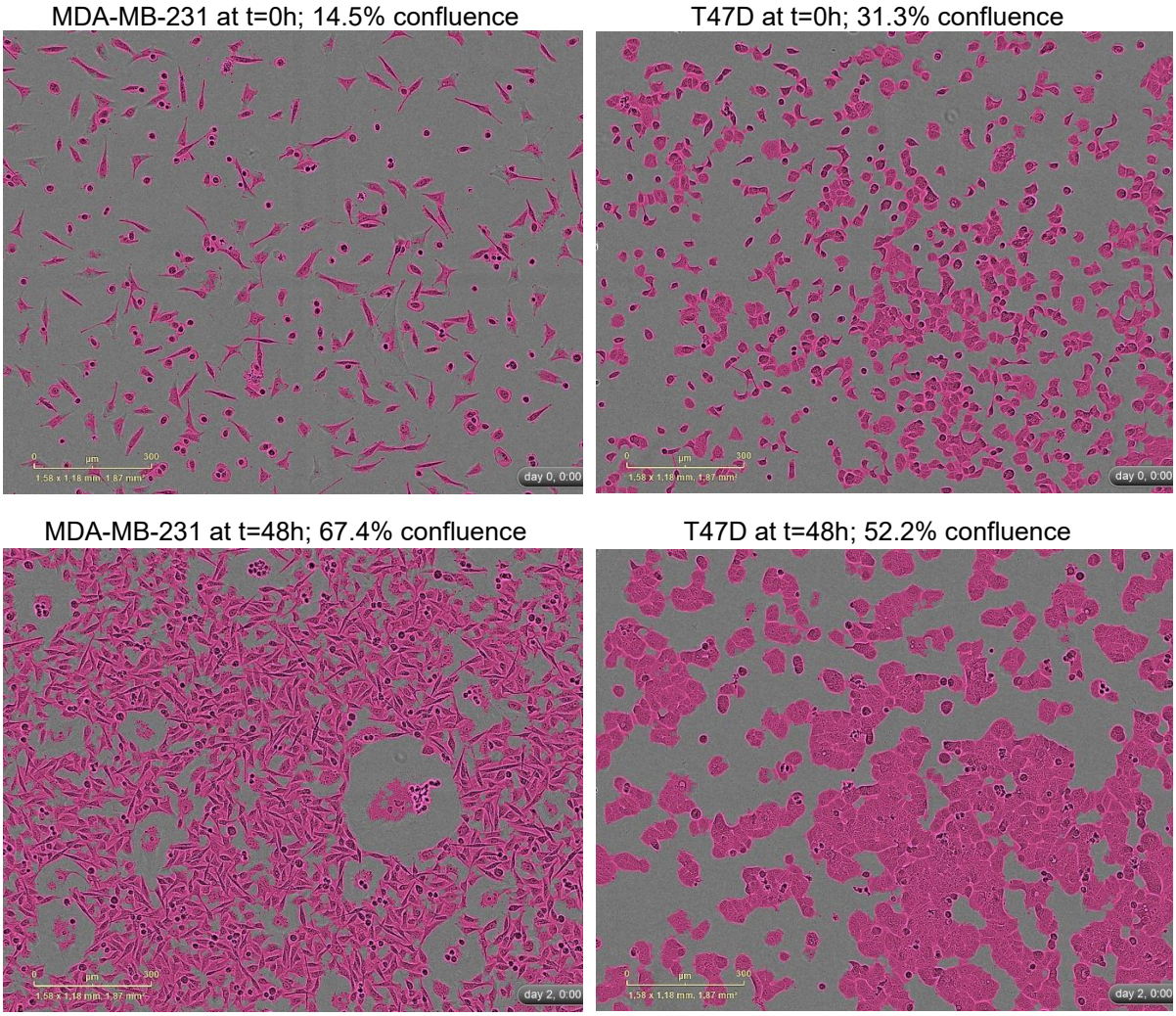

Figure 4. Incucyte images of both cell lines at 0h and 48h time points. The purple coloring corresponds to the confluence mask of the Incucyte analysis tool.

3.3.2 Selection of the experiment parameters

To determine the appropriate treatment groups and duration of cultivation, a preliminary experiment was performed. MDA-MB-231 cells and T47D cells were plated on four different culture plates (Incucyte® ImageLock 4379 96-well plates by Essen BioScience), 5 000 and 10 000 cells per well respectively. The cell numbers were selected based on the proliferation rates of the cell lines and preliminary proliferation data. The cells were cultivated in different concentrations of human lymph (10%, 30%, and 50%) in RPMI supplemented with GlutaMAX™ for either 0, 24, 48, or 72 hours. Proliferation was measured by CyQuant and Incucyte.

The concentration of 10% of lymph was chosen based on several considerations. First, in CyQuant analysis, there was some indication that especially T47D cells might not proliferate as well in 30% lymph, compared to 10% lymph. Second, at lymph concentrations of 30% and

50%, visibility in phase contrast microscopy was lost almost entirely, rendering Incucyte analysis unfeasible. Proliferation times of 48 and 68 hours were chosen for the MDA-MB-231 and T47D cell lines, respectively. According to Incucyte data, the proliferation of MDA-MB-231 cells started to plateau at around 80% confluence, or after 50 hours of cultivation with a starting population of 5000 cells. A similar plateau effect was not seen with T47D cells even after 72 hours of cultivation. The 68-hour time point for the T47D cell line was chosen for practical reasons as well as a compromise between the cell lines for CyQuant analysis as CyQuant analysis requires freezing of the whole culture plate.

3.4 Statistical methods

Descriptive statistics are shown with means and standard errors of means (SEMs). Mann-Whitney test was used to determine the statistical significance between Clever-1 depleted and mock depleted samples in both Incucyte and CyQuant datasets, because the normality assumption could not be estimated with n=3. A significance level of 0.05 was used.

Outliers in the technical replicates from the datasets of both experiments were estimated using the ROUT method[38]. Q (i.e., statistical significance) was set to 5 %. This resulted in only one outlier in one technical replicate in the CyQuant analysis of T47D-cells treated with mock depleted lymph (donor 2). The outlier persisted even with Q=1% and was thus excluded as no reasonable explanation for the outlier was found. A few technical replicants were also visually excluded from the Incucyte analysis, based on strikingly low starting point confluences, leading to unreliably low or high confluence fold changes.

GraphPad Prism version 9.5.0 was used in all statistical analyses.

4 Results

The confluence data measured by Incucyte® Zoom were converted into confluence fold changes and plotted on graphs. As seen in Figure 4, the confluence of the MDA-MB-231 cells increased exponentially into an approximately 4-fold confluence in 48 hours, except for the negative control group in which the confluence slightly decreased and signs of cell death were seen. The T47D cells had a similar but a little slower growth rate, leading to a little over 2-fold growth in confluence in 68 hours while a similar decrease in confluence was seen in the negative control group.

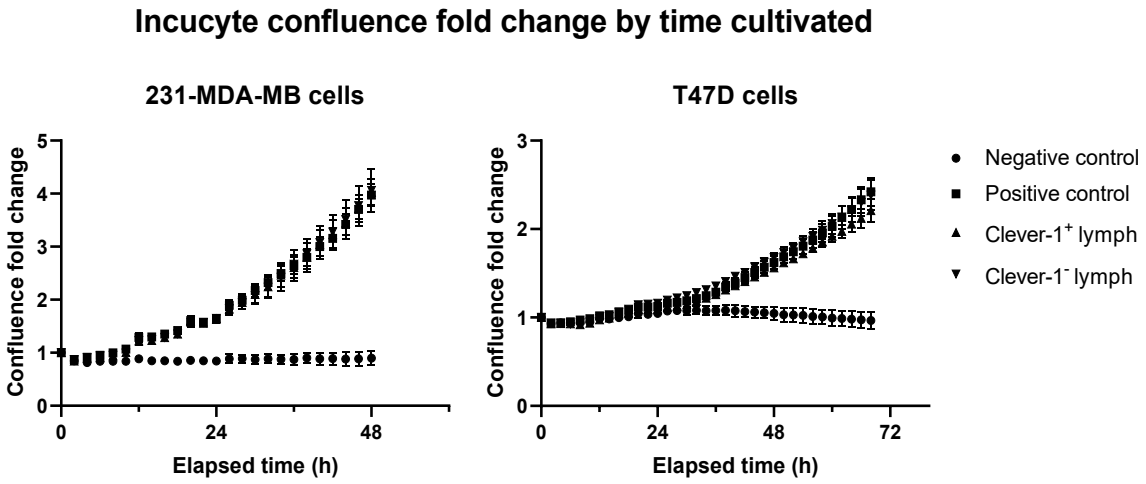

Figure 5. Confluence fold change of the MDA-MB-231 cells (left) and T47D cells (right) by the elapsed time between the different treatments up to 48 and 68 hours, respectively. Confluences were measured by Incucyte. The whiskers indicate standard errors of the means.

After 48 hours of culture, the MDA-MB-231 cells had mean confluence fold changes of 0.900 (SEM: 0.136), 3.97 (SEM: 0.199), 4.02 (SEM: 0.247), and 4.06 (SEM: 0.405) in the negative control, positive control, Clever-$1^{+,}$ and Clever-1^{-} treatment groups, respectively (Figure 6). Whereas the T47D cells had mean confluence fold changes of 0.966 (SEM: 0.0945), 2.42 (SEM: 0.160), 2.21 (SEM: 0.129), and 2.38 (SEM: 0.175) in the negative control, positive control, Clever-$1^{+,}$ and Clever-1^{-} treatment groups, respectively (Figure 6). There was no statistically significant difference between the Clever-1^{+} and Clever-1^{-} groups in either cell line (MDA-MB-231: $p>0.9999$; T47D: $p=0.70$).

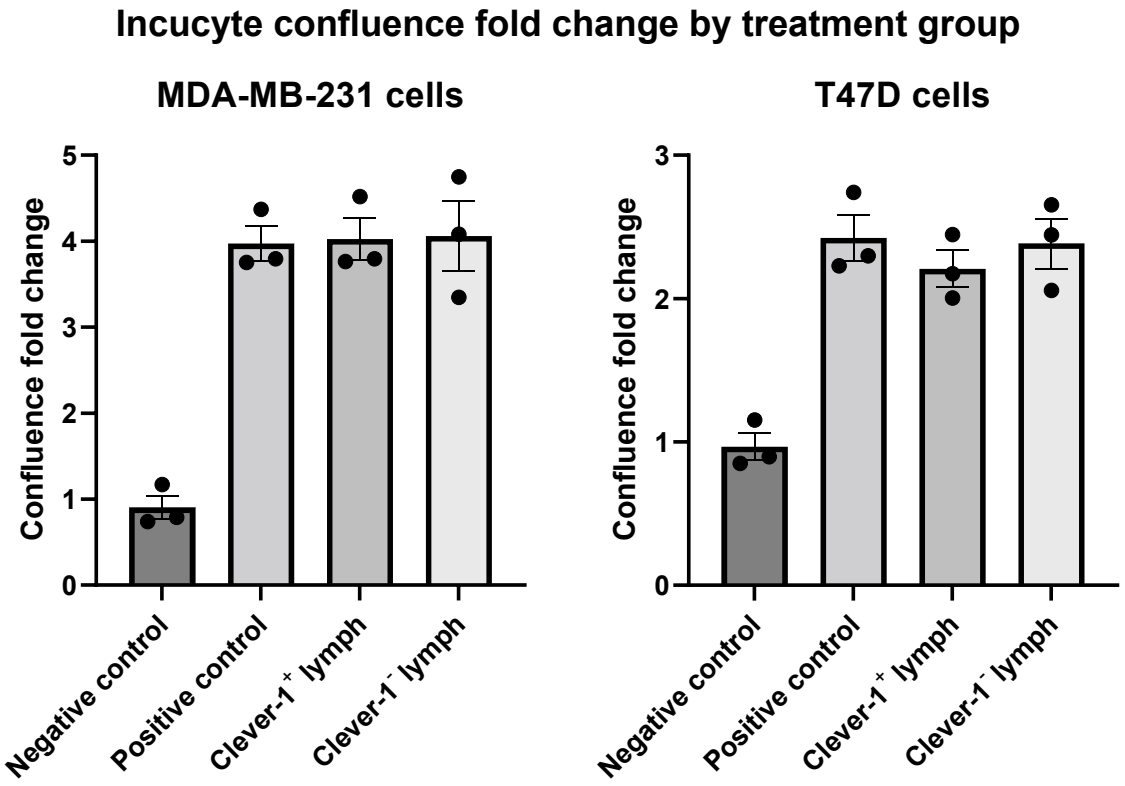

Figure 6. Comparison of endpoint confluence fold changes between the different treatments, measured by Incucyte. MDA-MB-231 cells (left) at 48 hours and T47D cells (right) at 68 hours. The whiskers indicate standard errors of the means.

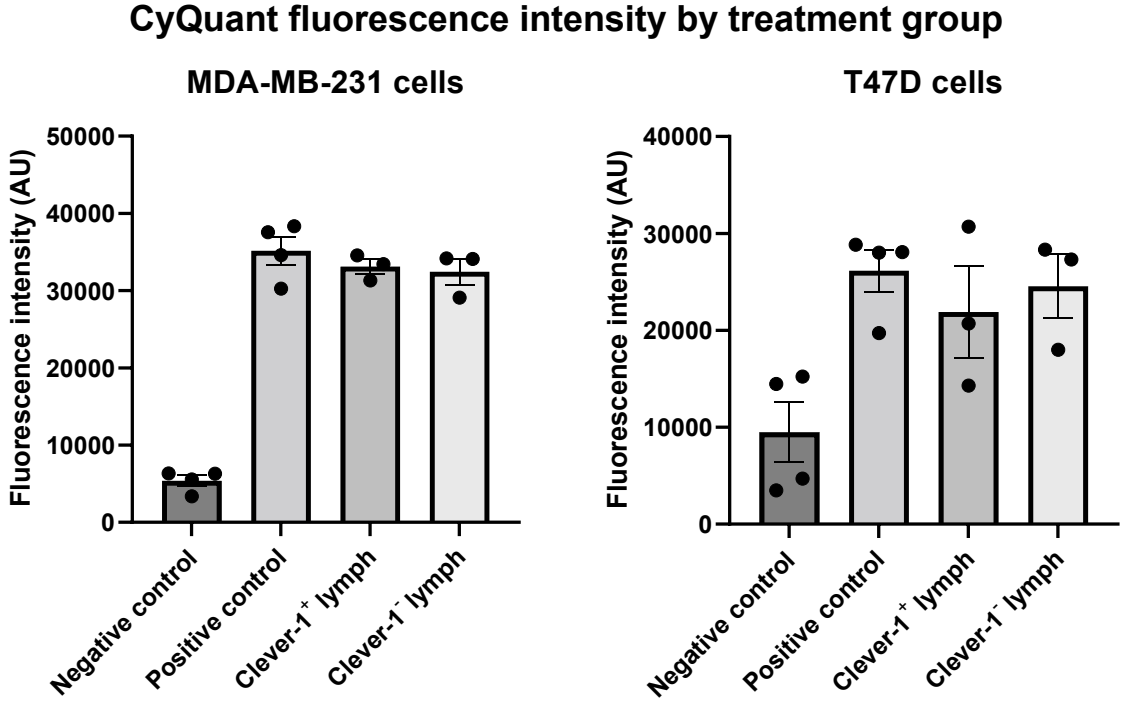

Figure 7. Comparison of fluorescence intensities of the differently treated CyQuant-samples. MDA-MB-231 cells (left) and T47D cells (right) after 68 hours of cultivation. The whiskers indicate standard errors of the means. AU = arbitrary units.

In CyQuant analysis (Figure 7), the MDA-MB-231 cells had mean fluorescence intensities of 5 390 (SEM: 698), 35 200 (SEM: 1 830), 33 100 (SEM: 950) and 32 500 (SEM: 1 680) arbitrary units (AU) in the negative control, positive control, Clever-$1^{+,}$ and Clever-1^{-} treatment groups, respectively. The mean fluorescence intensities of the T47D cells were 9470 (SEM: 3 120), 26 200 (SEM: 2 150), 21 900 (SEM: 4 780), and 24 500 (SEM: 3 290) AU in the negative control, positive control, Clever-$1^{+,}$ and Clever-1^{-} treatment groups, respectively. There was no statistically significant difference between the Clever-1^{+} and Clever-1^{-} treatment groups (MDA-MB-231: $p>0.9999$; T47D: $p>0.9999$).

5 Discussion

Cancer metastasis is a multi-step process in which not only circulating cancer cells, but blood vessels, immune cells, the lymphatic system, the primary tumor, and metastasis target organs interplay in a multilayer fashion. This study, while concentrating on one molecule, Clever-1, and its impact on cancer cell viability is a humble but important step in understanding the specific role of lymph in metastasis. In this study, the viability of breast cancer cells was estimated by measuring the proliferation of the cells. The results suggest that depleting soluble Clever-1 from lymph does not affect breast cancer cell proliferation *in vitro.* However, in addition to Clever-1, there are a plethora of other substances in human lymph, which might affect the results.

An interesting observation in this study was that the more aggressive MDA-MB-231 cells seem to thrive even in human lymph, much better than the T47D cells. Perhaps this could be explained by differing abilities in utilizing the components of lymph between the cancer cell lines, possibly due to differences in the cells' receptors.

The depletion of Clever-1 from the lymph succeeded remarkably well, and little to no residual Clever-1 remained. Another strength of this study was that the depletion was confirmed by two distinct methods: the in-house TRFIA of the Clever-1 depleted lymph and gel electrophoresis of the Clever-1 precipitate. We also showed that Clever-1 can be efficiently depleted from human lymph and breast cancer cells can be successfully cultured in a growth medium with FBS replaced by human lymph.

However, there were some limitations to this study. First, the proliferation duration used for the CyQuant analysis of the MDA-MB-231 cells was a little too long, resulting in slight plateauing in cell confluence and potentially lesser differences between the treatments. Additionally, only one time point was used, which means that the variance in the cell numbers pipetted into the wells cannot fully be accounted for. The other results, however, support the negative outcome, so this likely has no impact on the overall results. Second, approximately one-third of Clever-1 was lost even in mock depletion of the lymph, slightly reducing the relative effect of the Clever-1-depleted lymph. This should not pose a large problem as there were very low residuals of Clever-1 in the Clever-1-depleted batches of lymph, except for donor 3 lymph. As for donor 3 lymph, the Clever-1 depletion result was not as optimal as desired, which might be due to inadequate amounts of antibody-coated CNBr beads or a

human error in the depletion process. Third, there were challenges in getting the cells to distribute and attach evenly when plated on the cell plates. This might affect the reliability of the Incucyte results, as migration from a more confluent area into the Incucyte field of view might skew the data. To prevent data skewing, distinct outliers in the technical replicants were excluded. Finally, the T47D cells transform over time, which possibly explains why later datasets/experiments showed greater and faster proliferation regarding the T47D cells.

As mentioned before, there are a plethora of other substances in human lymph in addition to Clever-1, which might affect the results. Thus, a further study using recombinant Clever-1 could provide more insight. Also, further studies are required concerning the other important steps in cancer growth and metastasis, such as adhesion and transmigration. It also might be that soluble Clever-1 does not directly affect cancer cells, but might have a role in general immunosuppression, indirectly promoting metastasis. Furthermore, the role of Clever-1 in metastatic niches is still largely unknown and more studies on its possible role in the epithelial-to-mesenchymal transition, cancer cell dormancy, pre-metastatic niches, and immune checkpoints are required.

In conclusion, by depleting Clever-1 from the lymph of human donors, we were able to study the impact of soluble Clever-1 on the viability of breast cancer cells. The results of this study showed that there seems to be no relationship between soluble Clever-1 in lymph and the viability of breast cancer cells. This provides important preliminary information about the roles of soluble Clever-1 in metastasis. Further studies are required on the several other steps of metastasis. Additionally, by using recombinant Clever-1, other contents of lymph as confounding factors could be eliminated.

References

1. Sung H, Ferlay J, Siegel RL, Laversanne M, Soerjomataram I, Jemal A, et al. Global Cancer Statistics 2020: GLOBOCAN Estimates of Incidence and Mortality Worldwide for 36 Cancers in 185 Countries. CA Cancer J Clin. 2021;71(3):209–49.

2. Karizak AZ, Salmasi Z, Gheibihayat SM, Asadi M, Ghasemi Y, Tajbakhsh A, et al. Understanding the regulation of "Don't Eat-Me" signals by inflammatory signaling pathways in the tumor microenvironment for more effective therapy. J Cancer Res Clin Oncol. 2022 Nov 7;

3. Hollmén M, Figueiredo CR, Jalkanen S. New tools to prevent cancer growth and spread: a 'Clever' approach. Br J Cancer. 2020 Aug 18;123(4):501–9.

4. Luzzi KJ, MacDonald IC, Schmidt EE, Kerkvliet N, Morris VL, Chambers AF, et al. Multistep nature of metastatic inefficiency: dormancy of solitary cells after successful extravasation and limited survival of early micrometastases. Am J Pathol. 1998 Sep;153(3):865–73.

5. Paget S. The distribution of secondary growths in cancer of the breast. 1889. Cancer Metastasis Rev. 1989 Aug;8(2):98–101.

6. Psaila B, Lyden D. The metastatic niche: adapting the foreign soil. Nat Rev Cancer. 2009 Apr;9(4):285–93.

7. Lu X, Kang Y. Chemokine (C-C Motif) Ligand 2 Engages CCR2+ Stromal Cells of Monocytic Origin to Promote Breast Cancer Metastasis to Lung and Bone *. J Biol Chem. 2009 Oct 16;284(42):29087–96.

8. Qian BZ, Li J, Zhang H, Kitamura T, Zhang J, Campion LR, et al. CCL2 recruits inflammatory monocytes to facilitate breast-tumour metastasis. Nature. 2011 Jul;475(7355):222–5.

9. Qian B, Deng Y, Im JH, Muschel RJ, Zou Y, Li J, et al. A Distinct Macrophage Population Mediates Metastatic Breast Cancer Cell Extravasation, Establishment and Growth. PLOS ONE. 2009 Aug 10;4(8):e6562.

10. Weis SM, Cheresh DA. Pathophysiological consequences of VEGF-induced vascular permeability. Nature. 2005 Sep;437(7058):497–504.

11. Freire Valls A, Knipper K, Giannakouri E, Sarachaga V, Hinterkopf S, Wuehrl M, et al. VEGFR1+ Metastasis–Associated Macrophages Contribute to Metastatic Angiogenesis and Influence Colorectal Cancer Patient Outcome. Clin Cancer Res. 2019 Sep 13;25(18):5674–85.

12. Chen Q, Zhang XHF, Massagué J. Macrophage Binding to Receptor VCAM-1 Transmits Survival Signals in Breast Cancer Cells that Invade the Lungs. Cancer Cell. 2011 Oct 18;20(4):538–49.

13. Brownlie D, Doughty-Shenton D, Soong DY, Nixon C, Carragher NO, Carlin LM, et al. Metastasis-associated macrophages constrain antitumor capability of natural killer cells

in the metastatic site at least partially by membrane bound transforming growth factor β. J Immunother Cancer. 2021 Jan 1;9(1):e001740.

14. Kitamura T, Doughty-Shenton D, Cassetta L, Fragkogianni S, Brownlie D, Kato Y, et al. Monocytes Differentiate to Immune Suppressive Precursors of Metastasis-Associated Macrophages in Mouse Models of Metastatic Breast Cancer. Front Immunol [Internet]. 2018 [cited 2023 Feb 18];8. Available from: https://www.frontiersin.org/articles/10.3389/fimmu.2017.02004

15. Mirzapour MH, Heidari-Foroozan M, Razi S, Rezaei N. The pro-tumorigenic responses in metastatic niches: an immunological perspective. Clin Transl Oncol Off Publ Fed Span Oncol Soc Natl Cancer Inst Mex. 2022 Sep 22;

16. Kaplan RN, Riba RD, Zacharoulis S, Bramley AH, Vincent L, Costa C, et al. VEGFR1-positive haematopoietic bone marrow progenitors initiate the pre-metastatic niche. Nature. 2005 Dec;438(7069):820–7.

17. Lyden D, Hattori K, Dias S, Costa C, Blaikie P, Butros L, et al. Impaired recruitment of bone-marrow–derived endothelial and hematopoietic precursor cells blocks tumor angiogenesis and growth. Nat Med. 2001 Nov;7(11):1194–201.

18. Stacker SA, Williams SP, Karnezis T, Shayan R, Fox SB, Achen MG. Lymphangiogenesis and lymphatic vessel remodelling in cancer. Nat Rev Cancer. 2014 Mar;14(3):159–72.

19. Rauniyar K, Jha SK, Jeltsch M. Biology of Vascular Endothelial Growth Factor C in the Morphogenesis of Lymphatic Vessels. Front Bioeng Biotechnol [Internet]. 2018 [cited 2023 Feb 2];6. Available from: https://www.frontiersin.org/articles/10.3389/fbioe.2018.00007

20. He Y, Rajantie I, Pajusola K, Jeltsch M, Holopainen T, Yla-Herttuala S, et al. Vascular Endothelial Cell Growth Factor Receptor 3–Mediated Activation of Lymphatic Endothelium Is Crucial for Tumor Cell Entry and Spread via Lymphatic Vessels. Cancer Res. 2005 Jun 1;65(11):4739–46.

21. Dadras SS, Paul T, Bertoncini J, Brown LF, Muzikansky A, Jackson DG, et al. Tumor Lymphangiogenesis: A Novel Prognostic Indicator for Cutaneous Melanoma Metastasis and Survival. Am J Pathol. 2003 Jun 1;162(6):1951–60.

22. Rofstad EK, Galappathi K, Mathiesen BS. Tumor Interstitial Fluid Pressure—A Link between Tumor Hypoxia, Microvascular Density, and Lymph Node Metastasis. Neoplasia. 2014 Jul 1;16(7):586–94.

23. Dieterich LC, Ikenberg K, Cetintas T, Kapaklikaya K, Hutmacher C, Detmar M. Tumor-Associated Lymphatic Vessels Upregulate PDL1 to Inhibit T-Cell Activation. Front Immunol [Internet]. 2017 [cited 2023 Feb 15];8. Available from: https://www.frontiersin.org/articles/10.3389/fimmu.2017.00066

24. Ma Q, Dieterich LC, Ikenberg K, Bachmann SB, Mangana J, Proulx ST, et al. Unexpected contribution of lymphatic vessels to promotion of distant metastatic tumor spread. Sci Adv. 2018 Aug 8;4(8):eaat4758.

25. Palani S, Elima K, Ekholm E, Jalkanen S, Salmi M. Monocyte Stabilin-1 Suppresses the Activation of Th1 Lymphocytes. J Immunol. 2016;196(1):115–23.

26. Irjala H, Elima K, Johansson EL, Merinen M, Kontula K, Alanen K, et al. The same endothelial receptor controls lymphocyte traffic both in vascular and lymphatic vessels. Eur J Immunol. 2003 Mar;33(3):815–24.

27. Salmi M, Koskinen K, Henttinen T, Elima K, Jalkanen S. CLEVER-1 mediates lymphocyte transmigration through vascular and lymphatic endothelium. Blood. 2004 Dec 15;104(13):3849–57.

28. Adachi H, Tsujimoto M. FEEL-1, a novel scavenger receptor with in vitro bacteria-binding and angiogenesis-modulating activities. J Biol Chem. 2002 Sep 13;277(37):34264–70.

29. Karikoski M, Marttila-Ichihara F, Elima K, Rantakari P, Hollmén M, Kelkka T, et al. Clever-1/stabilin-1 controls cancer growth and metastasis. Clin Cancer Res. 2014 Dec 15;20(24):6452–64.

30. Ålgars A, Kemppinen L, Fair-Mäkelä R, Mustonen H, Haglund C, Jalkanen S. Stage i–iv colorectal cancer prognosis can be predicted by type and number of intratumoral macrophages and clever-1+ vessel density. Cancers. 2021 Dec 1;13(23).

31. Ammar A, Mohammed RAA, Salmi M, Pepper M, Paish EC, Ellis IO, et al. Lymphatic expression of CLEVER-1 in breast cancer and its relationship with lymph node metastasis. Anal Cell Pathol. 2011;34(1–2):67–78.

32. Tervahartiala M, Taimen P, Mirtti T, Koskinen I, Ecke T, Jalkanen S, et al. Immunological tumor status may predict response to neoadjuvant chemotherapy and outcome after radical cystectomy in bladder cancer. Sci Rep. 2017 Oct 4;7(1):12682.

33. Boström MM, Irjala H, Mirtti T, Taimen P, Kauko T, Ålgars A, et al. Tumor-Associated Macrophages Provide Significant Prognostic Information in Urothelial Bladder Cancer. PloS One. 2015;10(7):e0133552.

34. Viitala M, Virtakoivu R, Tadayon S, Rannikko J, Jalkanen S, Hollmén M. Immunotherapeutic Blockade of Macrophage Clever-1 Reactivates the CD8+ T-cell Response against Immunosuppressive Tumors. Clin Cancer Res Off J Am Assoc Cancer Res. 2019 Jun 1;25(11):3289–303.

35. Swartz MA. Immunomodulatory Roles of Lymphatic Vessels in Cancer Progression. Cancer Immunol Res. 2014;2(8):701–7.

36. Keydar I, Chen L, Karby S, Weiss FR, Delarea J, Radu M, et al. Establishment and characterization of a cell line of human breast carcinoma origin. Eur J Cancer 1965. 1979 May;15(5):659–70.

37. Sartorius CA, Groshong SD, Miller LA, Powell RL, Tung L, Takimoto GS, et al. New T47D Breast Cancer Cell Lines for the Independent Study of Progesterone B- and A-Receptors: Only Antiprogestin-occupied B-Receptors Are Switched to Transcriptional Agonists by cAMP1. Cancer Res. 1994 Jul 1;54(14):3868–77.

38. Motulsky HJ, Brown RE. Detecting outliers when fitting data with nonlinear regression - A new method based on robust nonlinear regression and the false discovery rate. BMC Bioinformatics. 2006 Mar 9;7.